BAMS Article

# The Global Satellite Precipitation Constellation

## Current Status and Future Requirements

Chris Kidd, George Huffman, Viviana Maggioni, Philippe Chambon, and Riko Oki

**ABSTRACT:** To address the need to map precipitation on a global scale, a collection of satellites carrying passive microwave (PMW) radiometers has grown over the last 20 years to form a constellation of about 10–12 sensors at any one time. Over the same period, a broad range of science and user communities has become increasingly dependent on the precipitation products provided by these sensors. The constellation presently consists of both conical and cross-track-scanning precipitation-capable multichannel instruments, many of which are beyond their operational and design lifetime but continue to operate through the cooperation of the responsible agencies. The Group on Earth Observations and the Coordinating Group for Meteorological Satellites (CGMS), among other groups, have raised the issue of how a robust, future precipitation constellation should be constructed. The key issues of current and future requirements for the mapping of global precipitation from satellite sensors can be summarized as providing 1) sufficiently fine spatial resolutions to capture precipitation-scale systems and reduce the beam-filling effects of the observations; 2) a wide channel diversity for each sensor to cover the range of precipitation types, characteristics, and intensities observed across the globe; 3) an observation interval that provides temporal sampling commensurate with the variability of precipitation; and 4) precipitation radars and radiometers in low-inclination orbit to provide a consistent calibration source, as demonstrated by the first two spaceborne radar–radiometer combinations on the Tropical Rainfall Measuring Mission (TRMM) and Global Precipitation Measurement (GPM) mission *Core Observatory*. These issues are critical in determining the direction of future constellation requirements while preserving the continuity of the existing constellation necessary for long-term climate-scale studies.

**KEYWORDS:** Precipitation; Rainfall; Snowfall; Satellite observations; Microwave observations; Instrumentation/sensors

https://doi.org/10.1175/BAMS-D-20-0299.1

Corresponding author: Chris Kidd, chris.kidd@nasa.gov

In final form 12 May 2021

**AFFILIATIONS: Kidd**—Earth System Science Interdisciplinary Center, University of Maryland, College Park, College Park, and NASA/Goddard Space Flight Center, Greenbelt, Maryland; **Huffman**—NASA/Goddard Space Flight Center, Greenbelt, Maryland; **Maggioni**—Sid and Reva Dewberry Department of Civil, Environmental, and Infrastructure Engineering, George Mason University, Fairfax, Virginia; **Chambon**—CNRM, Université de Toulouse, Météo-France, CNRS, Toulouse, France; **Oki**—Earth Observation Research Center, Japan Aerospace Exploration Agency, Ibaraki, Japan

Water is not only a fundamental element of the Earth system, but also vital to all life on Earth. Consequently, the observation and measurement of precipitation (rainfall and snowfall) on a global scale is crucial to our understanding of the Earth system while impacting society across many levels (Kirschbaum et al. 2017; Skofronick-Jackson et al. 2017). Precipitation provides a direct link between the global cycles of energy and water through constraining and enabling the exchange of energy (Trenberth et al. 2009) and is the primary control of many natural hazards such as droughts and floods (Vicente-Serrano et al. 2010; Kundzewicz et al. 2014). However, the variability of precipitation makes it difficult to fully capture the characteristics of precipitation (see sidebar). Conventional measurements made by rain (and snow) gauges are generally representative of a very small area close to each gauge (Kyriakidis et al. 2001; Lundquist et al. 2019). While surface-based weather radar observations have limitations (Harrison et al. 2000; Ciach and Krajewski 1999), they provide valuable spatial measurements over large areas, complementing the global coverage provided by gauge data. Crucially, over the oceans few or no observations are available (or possible) through conventional means (Kidd et al. 2017). Even fundamental questions, such as addressing the amount and occurrence of precipitation, are generally limited to land regions (e.g., Sun et al. 2006; Herold et al. 2016). Observations provided by satellite sensors are therefore key in the measurement of precipitation on a global scale (e.g., Adler et al. 2003). Since no single satellite can possibly achieve this coverage alone, a stable and robust constellation is critical for providing sufficient temporal sampling to capture the vagaries of precipitation, particularly in surface-data-sparse regions such as over the poles or oceans, to provide consistent global precipitation products to the user community (Huffman et al. 2007). Furthermore, long-term climate studies into changes in precipitation across the Earth's surface can only be achieved through maintaining such a constellation (Adler et al. 2017; Levizzani et al. 2018).

## Conventional precipitation measurements

***Gauge measurements.*** The de facto measuring device for precipitation is the rain (snow) gauge, typically consisting of a funnel and a collection vessel, but with a wide range of designs (Strangeways 2004; Sevruk and Klemm 1989). The amount of water collected is usually measured daily, but less often in more remote regions. Automatic recording of the rainfall is possible with, for example, tipping-bucket gauges, which record the time/date that a known quantity of rainfall tips a small bucket (Sevruk 2005). Gauges are, however, subject to errors and uncertainties in their measurements (Ciach 2003; Villarini et al. 2008). The primary error of gauge measurements results from turbulence around the gauge orifice (Duchon and Biddle 2010), which may cause significant undercatch in light rain and/or strong winds (Kochendorfer et al. 2017). Measuring snowfall is more problematic due to the lower fall speeds of snowflakes (Thériault et al. 2012), resulting in the use of "shields" around snow gauges to reduce the wind speed around the gauge orifice (Duchon and Essenberg 2001). Despite issues relating to their accuracy, gauges remain the mainstay of conventional global precipitation measurements, particularly when corrections are applied (Michelson 2004). Even so, their coverage across

## Precipitation Characteristics

The requirements for observing precipitation are driven by the very specific scale and characteristics that precipitation exhibits, creating a challenging statistical problem.

At the microphysical scale, water is the only element that coexists in all three phases, namely, vapor, liquid, and solid, a situation that is common in many precipitation systems. Liquid-phase water starts with the formation of water droplets (about 10 $\mu$m), usually on cloud condensation nuclei (~0.1 $\mu$m), through the growth of cloud droplets, to precipitation-sized particles (~100 $\mu$m, up to 4–5 mm). Smaller droplets are spherical, but large droplets become flatter or even umbrella-shaped due to air resistance prior to breakup. Pristine ice-phase water particles have similar growth, except physical aggregation of particles and interactions with liquid (riming) also occur. The resulting icy particles exhibit a vast range of shapes and sizes, with significant implications for the retrieval and estimation of (frozen) precipitation.

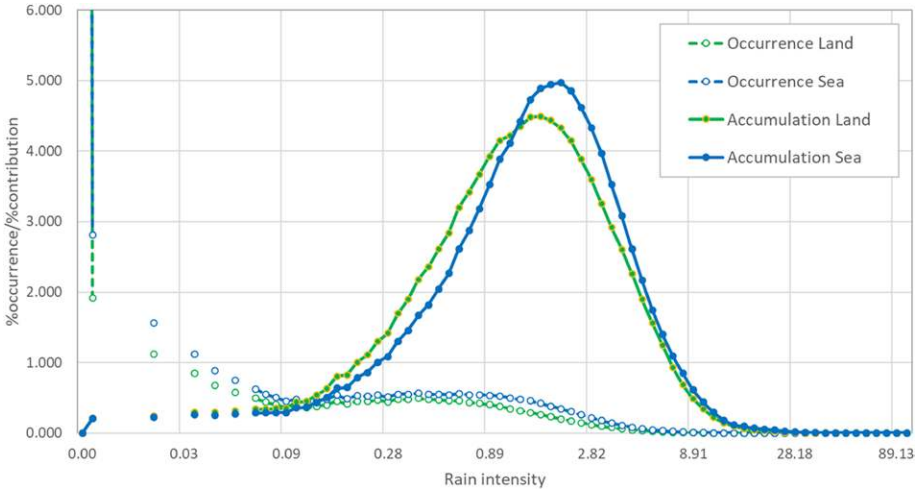


**Fig. SB1. Distribution of the occurrence/contribution of precipitation by intensity based upon instantaneous surface radar data over the United Kingdom (2014–19) at 15 km × 15 km resolution. Note that the precipitation intensity is plotted on a log scale; the occurrence of precipitation is highly skewed toward zero.**

At the precipitation system scale, the mechanisms driving the microphysical processes that form clouds and falling precipitation result in variations in precipitation that range from a few meters to 1,000 km or more and from a few seconds to days, weeks, and longer (Trenberth et al. 2009). Thus, the observation of precipitation is very much affected by interaction between the time/space scales of the rain being observed and the resolution/sampling of the observing system (Luini and Capsoni 2012).

The precipitation statistics in space/time are unusual in that the normal/modal value is zero: for most of the time and for the majority of the globe, it is not raining/snowing. Furthermore, when precipitation does occur, it is heavily skewed toward light precipitation intensities, while the accumulation of precipitation (being a function of occurrence times intensity) is more log-normally distributed (see Fig. SB1). As instantaneous samples are accumulated over time and space, the distribution shifts toward a more normal distribution. This complicates any statistical evaluation and requires extreme care when analyzing or evaluating precipitation datasets. Specifically, the distribution of precipitation intensities is very much dependent upon the spatial and temporal scales being considered (Luini and Capsoni 2012), such that observing a precipitation system at the same time with sensors with different spatial resolution will yield different results. Similarly, comparing instantaneous precipitation with precipitation accumulated over a few minutes, days, or months will reveal very different characteristics. The practical implication is that instantaneous point measurements cannot be directly compared with those collected over an area and/or over time. This issue in compounded by the fact that precipitation events tend to last for periods ranging from a few minutes to hours.

the globe is extremely variable. Over land, some regions have what could be considered adequate coverage, while other regions have none. Measurements over oceans are only available from a few atoll or island locations and a very small number of moored or drifting buoys. Overall, the global surface represented by gauge measurements is pitifully small (Kidd et al. 2017).

***Weather radar measurements.*** The technological development of weather radar systems has created an important source of information on precipitation at local to regional scales (Whiton et al. 1998a,b). Unlike the point measurements of gauges, radars can provide frequent, three-dimensional observations of precipitation up to about 250 km from the radar location (Zhang et al. 2011, 2016). However, radars rely upon several assumptions to convert the backscatter signal from rain and/or snow to an equivalent rain intensity

(Campos and Zawadzki 2000; Uijlenhoet 2001; Uijlenhoet et al. 2003). To avoid surface clutter the radar beam is usually elevated resulting in the altitude of the beam increasing with range, thereby no longer measuring surface precipitation and making near-surface phase (rainfall vs snowfall) detection difficult (Mimikou and Baltas 1996). Furthermore, quantitative radar measurements of precipitation are usually calibrated against gauge data where available, and due to the expense of installation, operation, and maintenance, weather radars tend to be clustered in developed countries, while their data may not be freely available.

***Emerging systems.*** Over the last few years, a number of new surface-based instruments and techniques have shown merit for measuring precipitation and augmenting conventional measurements, particularly in regions with few or no surface observations. Over the oceans precipitation data are particularly scarce, being limited to island gauges, buoys, or ships, and are typically not be representative of the open-ocean precipitation. Estimating rainfall through the use of underwater hydrophones is presented by Pumphrey et al. (1989), Medwin et al. (1992), and Forster (1994). More recently Ma and Nystuen (2005) found an excellent agreement between acoustic, gauge, and Tropical Rainfall Measuring Mission (TRMM) satellite measurements, particular at higher rain rates. While very promising, the expense for deployment and maintenance of such instrumentation is significant, although the rewards are likely to be great. Over land, the attenuation of microwave communication signals by rainfall has been studied since the late 1960s (see Semplak and Turrin 1969). This path attenuation can now be fully exploited due to the current widespread mobile phone infrastructure, as exemplified by the work by Leijnse at al. (2007) over the Netherlands. Since the microwave paths are close to the surface, they tend to be more representative of surface rainfall than weather radars. A more comprehensive study by Overeem et al. (2011) showed very good correlations between the link-derived estimates and those from the weather radar. Further development would complement and augment existing precipitation measurements in regions where few precipitation observations exist.

## Satellite precipitation measurements

***Satellite systems and retrievals.*** Precipitation-capable satellites may be classified by their orbit and sensing frequencies. Low-Earth-orbiting (LEO) satellites orbit between 400- and 800-km altitude, provide about 14–16 orbits per day, and typically operate in a sun-synchronous orbit. Some low-inclination, non-Sun-synchronous satellite orbits provide observations at different times of day as the orbits precess over periods of weeks or months. The LEO satellites sensors generally provide a broad subsatellite swath of data, although some only provide data over a narrow swath or only at nadir. The Cloud Profiling Radar (CPR) on *CloudSat* (Stephens et al. 2002, 2018), although not designed to retrieve precipitation, has shown significant merit in observing and estimating light precipitation. Despite the nadir-only observations of the CPR, its increased sensitivity has proved invaluable at providing an additional calibration/validation data source for precipitation retrieval schemes, particularly for light precipitation and snowfall (Battaglia et al. 2020). LEO satellites most relevant for precipitation studies carry visible (VIS), infrared (IR), passive microwave (PMW), and active microwave (AMW) sensors (Kidd and Levizzani 2011). Geostationary (GEO) satellites occupy a much higher orbit of about 35,800 km and are synchronized with the Earth's rotation so they appear stationary over a fixed location at the equator, allowing frequent and regular observations to be made. However, due to their altitude and requirements for sufficiently fine-resolution measurements, these observations are currently restricted to VIS/IR sensors. Mission concepts have been developed for geostationary PMW sensors (e.g., Tanner et al. 2007; Lambrigtsen et al. 2007; Duruisseau et al. 2017; Lambrigtsen 2019), but these typically

**Table 1. Characteristics of present-day LEO and GEO satellites and their observational capabilities.**

| | | | Orbit | |
|---|---|---|---|---|
| | | | LEO[a] | GEO[b] |
| | | Characteristics | 400–800-km-altitude orbits<br>~14–16 orbits per day<br>Polar-orbiting sun-synchronous (up to two overpasses per day), or low-inclination precessing orbits | ~36,000-km-altitude orbits<br>Geosynchronous orbit—satellite remains stationary relative to subsatellite point. |
| Observations by band | VIS/IR | Cloud-top properties<br>Reflection, emission, texture and particle sizes | Multispectral<br>Orbital swaths<br><1 m to 1 km | Multispectral<br>Frequent/regular samples over sectors or full disk coverage<br><1–4-km footprints at subsatellite point |
| | PMW | Hydrometeor column<br>Liquid, ice and water vapor | Multichannel<br>Orbital swath<br>~5–70-km footprints | *Not possible at present*<br>*Several feasibility studies* |
| | AMW | Vertical profiles of hydrometeors<br>Backscatter<br>Liquid, ice | Single/dual frequency<br>(13.6, 35, 94 GHz)<br>Single beam (*CloudSat* with 1.4 and 5.4 km footprints) or narrow swath (DPR 245 km swath and 5.4 km × 5.4 km footprints) | *Not possible at present*<br>*Some feasibility studies* |

[a] LEO: VIS/IR observations provided by a large group of sensors ranging from land surface monitoring missions (e.g., Landsat) through to meteorological missions (e.g., AVHRR) with resolutions typically matched to user requirements. PMW channels used for the retrieval of geophysical and meteorological parameters, including precipitation.

[b] GEO: Constellation of GEO satellites provides global coverage with frequent/regular observations, disseminated at a nominal 3-hourly interval, but with sensors typically providing operational 10–15-min data collection, and rapid scans < 1 min.

would only provide limited coverage at any one time and with limited frequencies. Table 1 summarizes the range of satellite observing systems.

Satellite observations for precipitation estimation extend back over 40 years, with the longest data records based upon VIS and/or IR imagery. Early precipitation estimates relied upon empirical relationships between the cloud top (brightness and/or temperature) characteristics and surface rainfall (Kidd and Levizzani 2011). However, this relationship is generally poor and inconsistent over time and space (Kidd and Muller 2010; Kidd and Levizzani 2019). PMW radiometers, developed in the mid-1970s, rely upon the upwelling radiation from the Earth's surface that is largely unaffected by the presence of cloud, particularly at the lower frequencies (below 37 GHz). Sufficiently large liquid and ice particles (as in the case of precipitation) affect the upwelling radiation, resulting in increased radiation at the lower frequencies due to emission from liquid droplets, while at the higher frequencies ice particles cause a decrease in the upwelling radiation (Kummerow 2020). Although PMW observations are more direct than those of the VIS/IR, many assumptions are necessary to convert the satellite observations into precipitation estimates, particularly over land, where low-frequency observations are impractical for retrieving precipitation. The most direct measure of precipitation from space is obtained from precipitation radars and relies upon the backscatter from the precipitation sized particles to estimate precipitation intensity in the same way as their ground-based counterparts (see Battaglia et al. 2020). Two precipitation-specific radars have flown; the first, the TRMM Precipitation Radar (PR) operated at 13.6 GHz (Kummerow et al. 1998) and the Global Precipitation Measurement (GPM) mission Dual-Frequency Precipitation Radar (DPR) operating at 13.6 and 35.5 GHz (Hou et al. 2014), while the cloud-orientated CPR operates

at 94 GHz. As with ground-based radars, the backscatter-to-precipitation relationship is not consistent, and they cannot retrieve precipitation within about 500–2,000 m of the surface due to clutter (Skofronick-Jackson et al. 2019).

On a global scale the satellite-based observations largely address the shortcomings of conventional measurements for observing precipitation while also providing data for studying the characteristics and mechanisms of precipitation (Tapiador et al. 2011). However, to measure and map precipitation correctly, satellite systems must provide sufficient sampling to capture the temporal and spatial variability of precipitation.

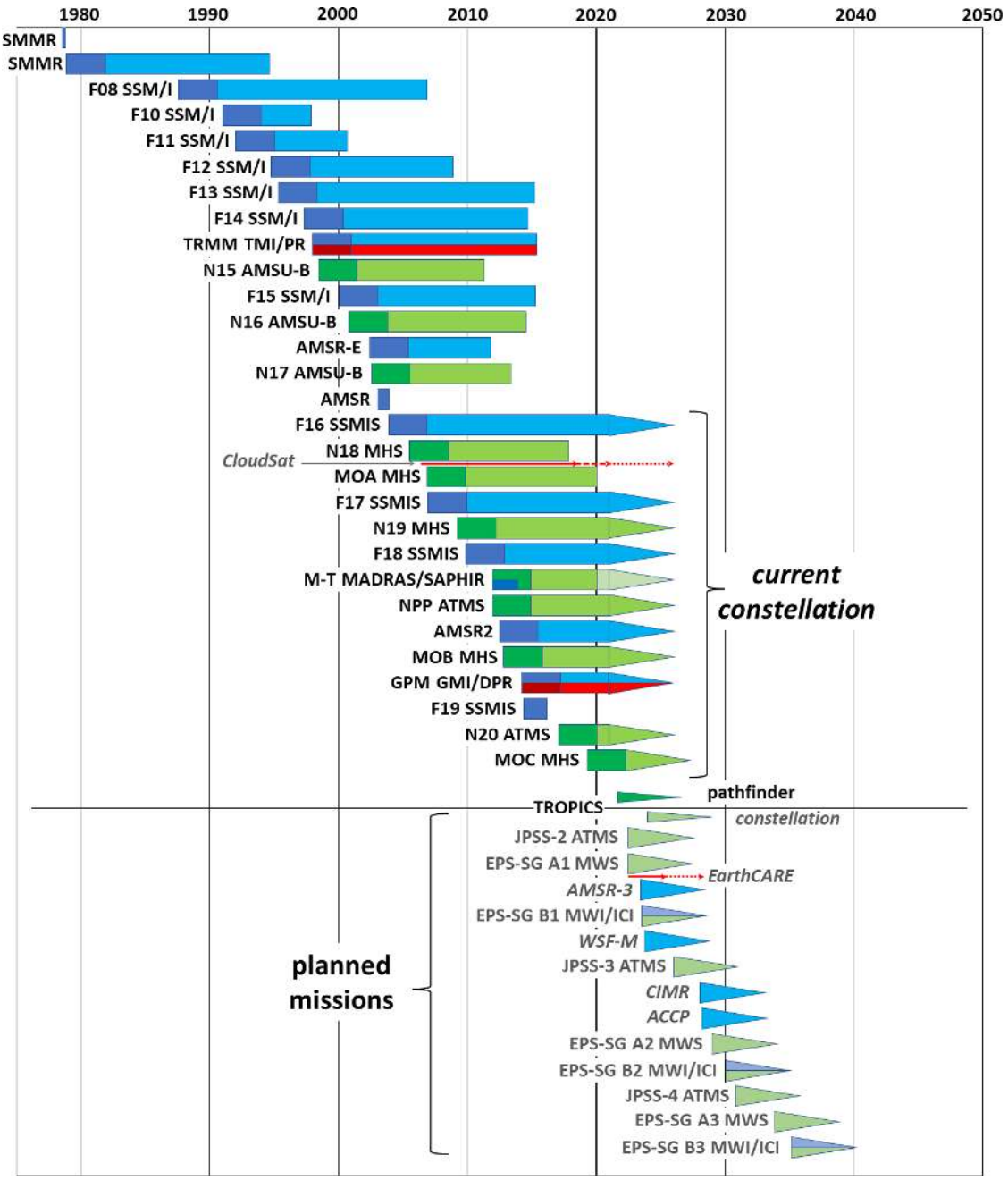


**Fig. 1. Timeline of PMW satellites and sensors providing analysis-ready data. The wide bars and arrows indicate swath-based and nadir-only observations, respectively. Blue bars represent imaging/conical scanning radiometers, green bars represent sounding/cross-track radiometers, and red bars indicate AMW (radar) sensors. Triangles indicate those sensors that currently provide data (as of 9 Feb 2021) and may continue to do so, together with future missions. [Data source: based upon World Meteorological Office (WMO) Observing Systems Capability Analysis and Review Tool (OSCAR) database and EUMETSAT.]**

***Current precipitation constellation.*** The evolution of the constellation of precipitation-capable sensors is shown in Fig. 1. Conically scanning PMW sensors began in the late 1980s, with cross-track-scanning PMW sounding instruments from the late 1990s onward. The latter, although primarily designed for retrieving temperature and humidity (Mo 1995), have proved valuable in increasing the temporal sampling necessary for precipitation measurements (Kidd et al. 2016, 2021; Bagaglini et al. 2021). The launch of TRMM (Simpson et al. 1988; Kummerow et al. 1998) in 1997 facilitated multisensor retrievals through the intercalibration of the then-available PMW sensors with the TRMM instruments. This intercalibration concept was expanded with GPM (Hou et al. 2014; Skofronick-Jackson et al. 2017), launched in 2014.

The GPM-CO carries the DPR and the GPM Microwave Imager (GMI), both of which have been shown to be very well calibrated (Wentz and Draper 2016). Alongside the GPM-CO, a constellation of about 10–12 PMW-based precipitation-capable satellites is provided by several international agencies (see Table 2). Among these are the operational missions of NOAA (with the MHS and ATMS sensors), EUMETSAT (MetOp MHS), and the U.S. Department of Defense (DoD) SSMIS sensors (Kidd et al. 2020). In addition, JAXA contributes the AMSR-2, while the Centre National d'Etudes Spatiales (CNES) and the Indian Space Research Organization (ISRO) contribute SAPHIR from the Megha-Tropiques mission (Roca et al. 2015). Data archives of the observations from all of these and previous PMW missions provide the necessary input for routine global estimates throughout the entire record. Additional operational precipitation capable PMW missions exist (e.g., Li et al. 2018), but due to data access/usage arrangements these cannot yet be fully exploited by the wider precipitation community. The multiagency coordination of the orbital crossing times of these missions affects the temporal sampling. For example, at present the EUMETSAT, NOAA, and JAXA missions generally use station-keeping to ensure consistent overpass times, while the crossing times of other PMW satellites drift over the course of 14–15 years between the extremes of ~1330–2230 LT (ascending node). A number of missions (i.e., TRMM, GPM, and Megha-Tropiques) had, or have, non-sun-synchronous precessing orbits and therefore observe the full diurnal cycle at any one location over the period of a few months, albeit with highly intermittent sampling (Roca et al. 2018).

In addition to the PMW sensors, a ring of GEO satellites provides frequent and regular VIS/IR observations (see Table 3) that are used to augment the LEO PMW observations. These satellites' IR data are used as input for the NOAA Climate Precipitation Center (CPC)

**Table 2. Microwave sensors contributing to the GPM precipitation constellation. The current precipitation constellation missions are highlighted in boldface. An asterisk indicates the retrieval resolution is that of the NASA GPROF scheme.**

| Satellite | Agency | Sensor/number | | Channels | Retrieval resolution |
|---|---|---|---|---|---|
| ***AMW instruments*** | | | | | |
| **GPM** | **NASA/JAXA** | **DPR** | **×1** | **13.6, 35.5 GHz** | **5.4 km × 5.4 km** |
| TRMM | NASA/JAXA | PR | | 13.6 GHz | 4.3 km × 4.3 km |
| ***PMW imagers*** | | | | | |
| **GPM** | **NASA/JAXA** | **GMI** | **×1** | **10.7–183.31 GHz** | **10.9 km × 18.1 km*** |
| ***DMSP F16, -17, -18, -19*** | **U.S. DoD** | **SSMIS** | **×3** | **19.35–183.31 GHz** | **45 km × 74 km*** |
| **GCOM-W1** | **JAXA** | **AMSR2** | **×1** | **6.7–89.0 GHz** | **14 km × 22 km*** |
| TRMM | NASA/JAXA | TMI | | 10.7–89.0 GHz | 20.9 km × 34.6 km* |
| ***PMW sounders*** | | | | | |
| ***NOAA-18, -19; MetOp-A, -B, -C*** | **NOAA/EUMETSAT** | **MHS** | **×3** | **89.0–183.31 GHz** | **17.12 km × 21.64 km*** |
| **NPP, *NOAA-20*** | **NOAA** | **ATMS** | **×2** | **23.0–183.31 GHz** | **16.51 km × 16.22 km*** |
| ***MeghaTropiques*** | **ISRO/CNES** | **SAPHIR** | **×1** | **183.31 GHz (×6)** | **7.34 km × 7.27 km** |

**Table 3. Current GEO VIS/IR sensors. Those that actively contribute to the global 30-min, 4-km IR imagery are highlighted in boldface. (All of these provide multichannel VIS/IR observations with temporal sampling of 15 min or better and spatial resolutions of <1 km for VIS and <4 km for IR at the subsatellite point).**

| Satellite | Agency | Sensor | Lon | Channels/number | | Subsatellite resolution |
|---|---|---|---|---|---|---|
| *GOES-13* (storage) | NOAA | Imager | 60°W | VIS/IR | × 5 | 1 km/4 km |
| *GOES-14* (backup) | NOAA | Imager | 105°W | VIS/IR | × 5 | 1 km/4 km |
| *GOES-15* (GOES-West backup) | NOAA | Imager | 128°W | VIS/IR | × 5 | 1 km/4 km |
| ***GOES-16* (GOES-East)** | **NOAA** | **ABI** | **75.2°W** | **VIS/IR** | **× 16** | **0.5 km/2 km** |
| ***GOES-17* (GOES-West)** | **NOAA** | **ABI** | **137.2°W** | **VIS/IR** | **× 16** | **0.5 km/2 km** |
| ***Meteosat-8* (IODC)** | **EUMETSAT** | **SEVIRI** | **41.5°E** | **VIS/IR** | **× 12** | **1 km/3 km** |
| *Meteosat-9* (rapid scan) | EUMETSAT | SEVIRI | 3.5°E | VIS/IR | × 12 | 1 km/3 km |
| *Meteosat-10* (rapid scan) | EUMETSAT | SEVIRI | 9.5°E | VIS/IR | × 12 | 1 km/3 km |
| ***Meteosat-11*** | **EUMETSAT** | **SEVIRI** | **0°** | **VIS/IR** | **× 12** | **1 km/3 km** |
| ***Himawari-8*** | **JMA** | **AHI** | **140.7°E** | **VIS/IR** | **× 16** | **0.5 km/2 km** |
| *Himawari-9* (standby) | JMA | AHI | 140.7°E | VIS/IR | × 16 | 0.5 km/2 km |

4-km, 30-min global IR composite (Janowiak et al. 2001) and the GridSat collection at 10-km, 3-h subsampled data (Knapp and Wilkins 2018) that are often used for precipitation retrievals in conjunction with the LEO PMW observations. Merged PMW and IR satellite schemes such as the CMORPH (Joyce and Xie 2011), GSMaP (Kubota et al. 2020), and IMERG (Huffman et al. 2020) allow precipitation products to be generated at resolutions of 30 min and 10 km or better, which critically relies upon sufficient high-quality PMW instantaneous retrievals of precipitation.

One of the pressing issues of the current constellation is the age of the satellite missions. It is fortuitous that many of the precipitation-capable missions have lasted beyond their designed operational lifetime with their respective agencies providing support to keep them

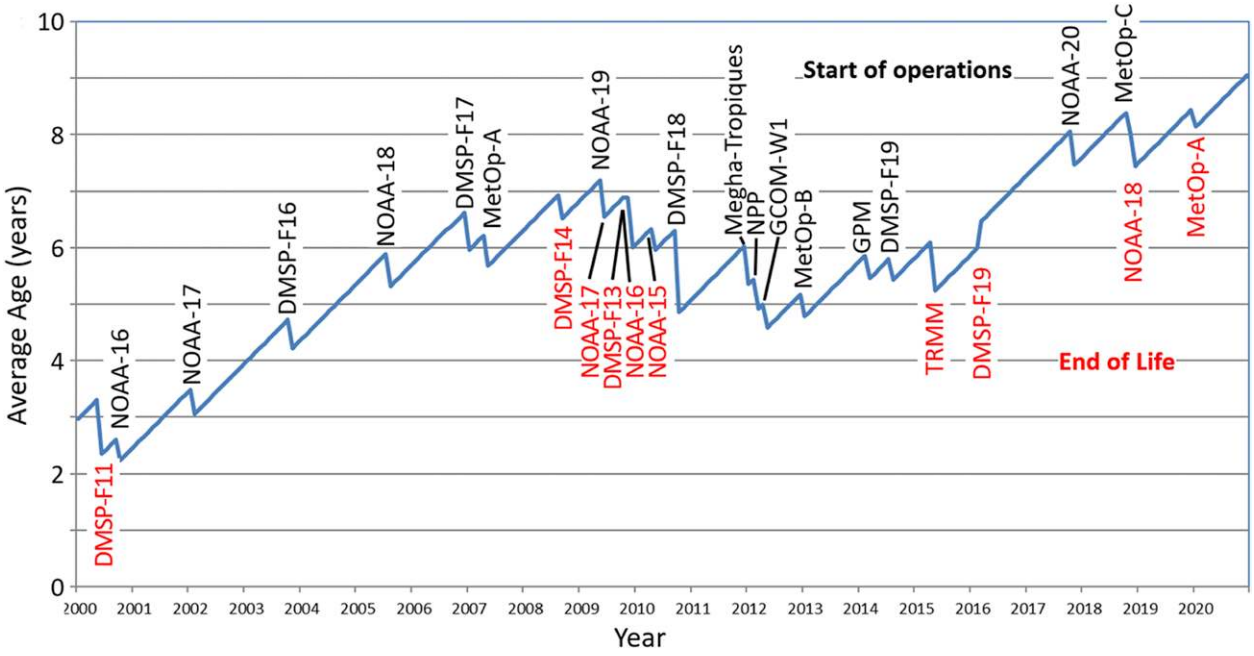


**Fig. 2. Mean age of the PMW satellites up to 1 Jan 2021. From 2005 to 2016 the mean age was around 5–7 years, but now currently exceeds 9 years. Note that the constellation becomes younger both with a new launch and if a long-term mission reaches its end of life.**

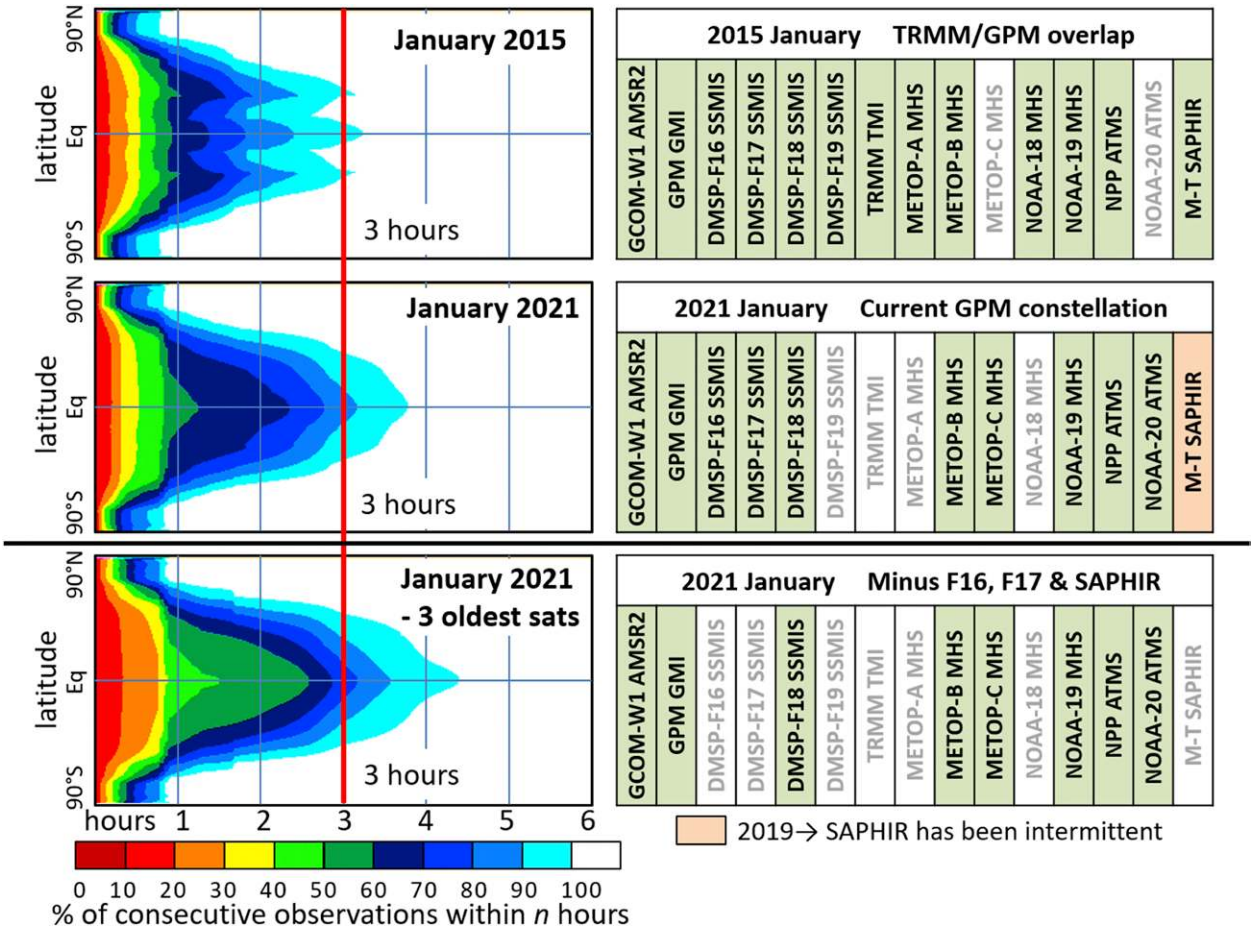


**Fig. 3. Comparison of the revisit times by latitude for three selected dates: (top) the baseline sampling of the GPM mission for January 2015 and (middle) the current sampling for January 2021. (bottom) A possible scenario if data from the three oldest sensors (SSMIS *F16* and *F17*, and SAPHIR) are not included. The red vertical line represents the widely accepted 3 h minimum revisit time necessary to adequately capture the accumulation of precipitation at daily, 0.25° scales. While the 3 h revisit time was attained more than 90% of the time in January 2015, the reduction in the constellation numbers has reduced this to about 80% in January 2021.**

operating. However, before 2016 the mean age of these satellites was 5–7 years; after 2016 the age has slowly risen and now is over 9 years (see Fig. 2). Crucially, satellites fail and sensors fail, often unexpectedly. A practical consequence of the gains and losses of these sensors is the direct impact upon the temporal sampling by the constellation. For example, a failure of the three oldest sensors in the constellation (the SSMISs on the DMSP *F16* and *F17* and the SAPHIR on *Megha-Tropiques*) would lead to a loss in the temporal sampling, extending the gaps between successive PMW observations, including the critical longest gaps, as illustrated in Fig. 3. A concerted program of new satellites/sensors is therefore necessary to ensure the adequate continuation of precipitation measurements in a controlled and planned manner to support the user requirements discussed below.

***Planned precipitation-capable missions.*** Going forward, there are several planned satellite missions that are capable of providing observations from which precipitation may be retrieved (see Fig. 1). The precipitation-capable missions planned for launch over the next decade include the following:

- EUMETSAT: The European Polar-Orbiting System (EPS) Second Generation (SG) will provide continuity to the current MetOp series of satellites, and so the orbital characteristics are

likely to be commensurate with the current missions, including station keeping (Accadia et al. 2020). The SG-A satellites will carry the cross-track Microwave Sounder (MWS; 24 bands, 23–229 GHz, 40–17-km resolution), while the SG-B satellites will carry the conically scanning Microwave Imager (MWI; 18 bands, 18.7–183 GHz, 50–10-km resolution; Accadia et al. 2020) and the Ice Cloud Imager (ICI; 11 bands, 183–664 GHz, 16-km resolution; Eriksson et al. 2020). The SG-A and SG-B satellites are likely to be in the same orbital plane but half-orbit offset allowing adjacent swath coverage. Precise launch dates are yet to be determined, but likely to be begin in the 2022–23 timeframe.

- NOAA: Additional members of the current Joint Polar System Satellite (JPSS) series (JPSS-2/-3/-4) through the 2030s are likely to occupy the same orbit as NPP and *NOAA-20* (Goldberg et al. 2013). Each will carry the ATMS sensor (22 band, 23–183 GHz), with resolutions on the order of 16 km at nadir for the higher-frequency channels, although the resolution at 88.2-GHz channel is 32 km.
- U.S. Department of Defense: The DoD has a long history of precipitation-capable missions (SSM/I and SSM/IS), and DoD has commissioned Ball Aerospace to build a new PMW imager: the Weather Satellite Follow-on–Microwave (WSF-M; see Newell et al. 2020). The planned sensor is a 6-frequency, 17-channel radiometer covering frequencies between 10 and 89 GHz with a finest spatial resolution of 15 km × 10 km. The contractual launch date is set as October 2023.
- JAXA: The third generation of the Advanced Microwave Scanning Radiometer (AMSR-3) sensor (Kasahara et al. 2020) is being built for installation on JAXA's Global Observation Satellite for Greenhouse Gases and Water Cycle (GOSAT-GW) with a scheduled launch date in 2023. The AMSR-3 sensor provides similar channel selection as the other AMSR sensors (12 channels, 6.7–89 GHz), but with additional higher-frequency channels at 166 and 183 GHz.
- NASA: Time-Resolved Observation of Precipitation Structure and Storm Intensity with a Constellation of Small Satellites (TROPICS) is a NASA Earth Venture Mission, providing six (plus one pathfinder) cubesats, primarily focused on the evolution of weather systems across the tropics (Blackwell et al. 2018). Each cubesat carries a small microwave radiometer operating at frequencies between 90 and 204 GHz with spatial resolutions similar to the MHS/ATMS sensors, and thus should be capable of providing observations for precipitation retrievals. An initial pathfinder mission was launched in 30 June 2021.
- China Meteorological Administration (CMA): The FY series of satellites carrying the Microwave Humidity Sounder-2 (MWHS-2) and the Microwave Radiation Imager (MWRI) instruments (Guo et al. 2015; Lawrence et al. 2018) has a proven record of precipitation-capable missions. The planned Chinese rain mapping missions (FY-3I and FY-3J) are expected to have capabilities similar to the GPM Core Observatory, hosting the PMW MWRI/MWHS-2 sensors and a rain radar providing observations at 13.6 and 35.5 GHz, and are currently planned to launch in 2022–23.

Other missions of interest being developed include the European Copernicus Imaging Microwave Radiometer (CIMR; Accadia et al. 2020); the ESA Arctic Weather Satellite (AWS) and EarthCARE; and the NASA-led Aerosols, Clouds, Convection, Precipitation mission (ACCP), which should be available for launch within the next decade. The Russian Meteor-N series also host both PMW imagers and sounders, although with limited data access. Many other small satellite missions (cubesats and smallsats) are proposed that could provide precipitation-relevant data (see Stephens et al. 2020). However, it is vital that such innovations support the spatial, temporal, channel, and quality requirements to address the needs of the user community, as well as facilitate the integration of their observations into the near-real-time production of satellite precipitation products.

## Defining future mission requirements

***User requirements.*** The main drivers for all new missions are a necessary compromise between the requirements of the user communities, the engineering/physical constraints, and the available budget. For precipitation, the temporal and spatial resolutions for the observations (and hence derived products) is determined by the capabilities of the observing system and the needs of the user communities and their applications. Polls of the user community found significant variations in the requirements of temporal and spatial sampling, as well as the latency (observation-to-delivery delay) [see Table 4 and Fig. 2 in Friedl (2014)] that depend on a huge range of research and application topics. Perhaps the most stringent requirements were associated with emergency managers, who require good spatial resolution (20 km or better) and frequent (every few minutes) and immediate (within a few minutes) information. For comparison, products from the current constellation using combined PMW and IR observations provide products at ~10-km resolution, every 30 min, within about 4 h, although very near-real-time IR-only products are available with reduced veracity. Importantly, the requirements within each user community are very diverse, and moreover, the scales may vary within a particular application, as demonstrated by Reed et al. (2015), who investigated the temporal sampling of precipitation datasets for hydrological modeling to meet the necessary flood-forecasting requirements. In that study, catchments with fast (slow) runoff characteristics require information more (less) frequently. Consequently, it is important to address the most stringent requirements as these are often those which have the greatest impact on both the physical and human environment, although in reality, the available scales and sampling are often coarser than the physical scales of precipitation and are further constrained by the physics and engineering of the sensors.

### *Addressing the temporal sampling and spatial resolution.*

**Spatial resolution at microwave frequencies.** Spatial resolution at microwave frequencies is essentially limited by the size of the antenna (dish) that can be deployed, which is driven by current-generation engineering, launch vehicle, and budget limitations. For a given antenna size, the best available resolution is inversely related to the observation frequency, meaning high-frequency channels have finer resolution than low-frequency channels for the same sized antenna. At present, the finest PMW resolution is about 3 km × 5 km at 89, 166, and 183 GHz using a 2-m dish (e.g., the GMI). Utilization of a larger dish is extremely problematic, both in terms of launch, and in terms of operation since the dish is continually rotating. Deployments of large (5–6 m) mesh antennas are planned, such as the CIMR mission (Accadia et al. 2020), but are limited to the lower-frequency channels (<37 GHz) by the current-generation limits to dish surface conformance. While GEO-based synthetic aperture systems have been studied for precipitation missions (e.g., Lambrigsten 2019), they require significant additional processing, are not truly global and envisage having only high-frequency channels. Thus, they presently do not necessarily provide significant advantage over LEO-based radiometers. Since the spatial variability of precipitation is on the order of a few kilometers, resolving this variability at 1 km or less would be ideal for satisfying the more stringent user needs, and remains a significant and unmet challenge.

**Temporal sampling from LEO satellites.** Temporal sampling from LEO satellites is constrained not only by the physical number of satellite sensors, but also by the swath over which each sensor collects data. For example, the AMSR2 sensor (Imaoka et al. 2010) collects data across a 1,450-km swath, while the GMI has a swath of 885 km. Temporal sampling of 3 h is often quoted as a minimum requirement. This was originally based upon the number of samples necessary to reduce ambiguities when observing the diurnal cycle of precipitation (by providing at least the first three sinusoidal components), as well as being inherited from intermediate and synoptic hours (0000 UTC, 0300 UTC, etc.), which has been the basis for the WMO-agreed

distribution of near-real-time GEO IR imagery. However, 3-hourly observations cannot adequately capture the true precipitation accumulation at the daily scale, as illustrated in Fig. 4. At 1 km an accumulation of the 3-hourly sampled data attains a correlation of less than 0.5 against the daily precipitation total and, while coarser resolutions provide higher correlations, even at 25-km resolution this does not exceed 0.8. This issue is further emphasized in Fig. 5, which shows the correlation of instantaneous PMW and IR estimates of precipitation against surface radar over the course of 1 day (25 July 2015) over the central United Kingdom. Each peak in the correlation represents the retrieval at a PMW sensor overpass. While the correlations between the satellite and surface radar products are good across all the satellites at the time of overpass, the correlation (in common with other measures) quickly deteriorates at times away from the time of the overpass. Even when the IR data are directly calibrated with the surface radar, as is done for Fig. 5, the PMW products are much better. Despite a reasonable number of PMW overpasses being available (as is currently the situation), there are clear gaps (around 0500 and 2300 UTC) on this day where no PMW overpasses occur and satellite precipitation estimates typically have to rely more heavily upon IR data.

## Strategies for maintaining a robust constellation

The current precipitation constellation provides a significant number of observations to generate precipitation estimates, but the continuity of these observations is very precarious. Historically, the precipitation community has become very adept at collecting observations from a diverse range of satellite missions and sensors, often not originally designed for the retrieval of precipitation, as well as incorporating information from other water-related missions to help close the water-cycle loop (Brocca et al. 2014; Behrangi 2020), but there is presently no adequate substitute for a steady supply of precipitation-relevant observations. To ensure a continuation of precipitation measurements from satellite systems, a number of strategies need to be considered.

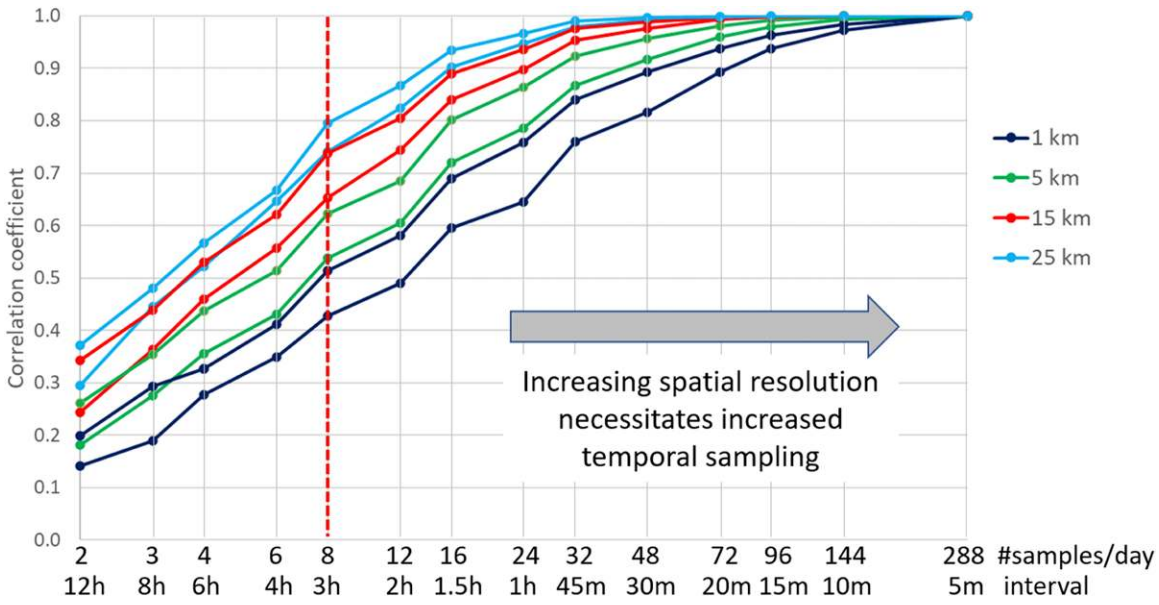


**Fig. 4. Correlation between temporally subsampled 5-min, 1-km radar data and the daily total (accumulating all 5-min samples) for two 300 km × 300 km areas (for each resolution) over the central United Kingdom during 2019. Despite the different relationships within each resolution category due to regional variations in precipitation characteristics, the general trend is that finer spatial resolutions require more samples. Note that for the nominal 3-hourly sampling (8 samples per day) the correlation is only between 0.4 and 0.5 at 1 km resolution and no better than 0.8 at 25-km resolution.**

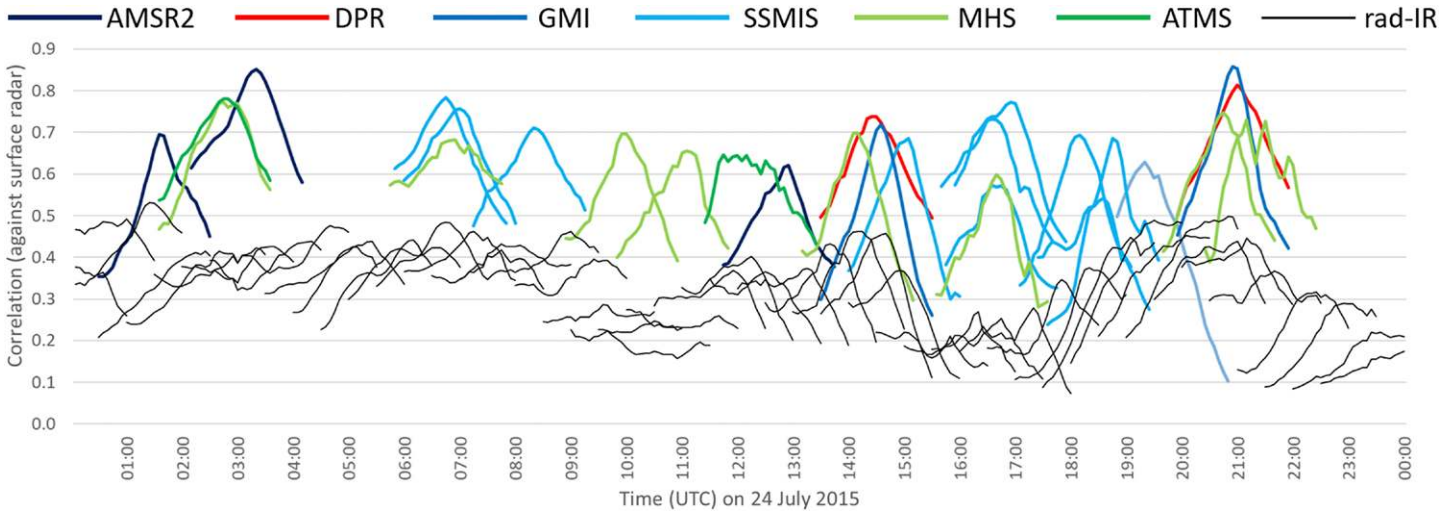


**Fig. 5. Correlation of satellite precipitation retrievals from IR, passive, and AMW sensors against surface radar for 24 Jul 2015 over the central United Kingdom. Each line segment covers a window over which the satellite estimate is compared with radar data up to ±1 h centered on the observation time of the satellite sensor. The microwave measurements generally have a good correlation at overpass time, but this falls quite quickly on either side of the observation time. The estimates derived from the radar-calibrated 30-min IR data are much poorer (rad-IR), as shown by the thin black lines.**

***Maintaining/strengthening the constellation through new missions.*** This is undoubtedly the largest driver for maintaining the capabilities of the precipitation constellation. The current constellation is continuously aging, with many of the current sensors now more than 10 years old, well beyond their anticipated mission lifetime (see Fig. 2). Given the length of time required to design, build, test and launch new sensors it is imperative that a long-term strategy for the constellation be devised and implemented. As discussed in the "Planned precipitation-capable missions" section, several operational missions are planned, such as the NOAA JPSS series, and the EUMETSAT EPS-SG series, but there are fewer dedicated long-term precipitation-specific missions with mapping capabilities. While many operational missions provide valuable observations for the precipitation community, such satellite sensors are not necessarily optimized for precipitation retrievals, nor do the orbital characteristics provide the frequent or uniform sampling necessary to capture the variability of precipitation. Observing System Simulation Experiments (OSSE) could be used (e.g., Chambon et al. 2014) to improve coordination between the satellite agencies is necessary to provide an optimal sampling strategy. Studies have been undertaken to assess the likely impact of the loss of one or more sensors within the constellation (Chambon et al. 2013).

***Robustness through redundancy.*** Larger satellites are generally more robust at dealing with failures due to built-in redundancy, allowing multidecadal records of observations to be collected, as in the case of TRMM. The long-term reliability of precipitation-capable cubesats and smallsats has yet to be fully evaluated, but it is anticipated that the orbital characteristics would determine the mission lifetime rather than system failure. Many operational meteorological satellites, such as the GEO missions (GOES, Meteosat, etc.) and the MetOp and NOAA polar-orbiting missions have on-orbit backup sensors. However, when the backup satellites continue to collect data while the primary satellite is functioning, they generally do so over the same space/time domains of the primary missions and therefore contribute relatively modestly to the overall temporal sampling.

***Extended mission lifetimes.*** Allowing missions to continue past their design lives and to continue contributing to the precipitation constellation is a proven concept. However, the

extension of missions is often fraught with obstacles, not least being the need to comply with the modern standards for end-of-life disposal of satellites to avoid space junk (Crowther 2002; Witze 2018). On a positive note, the precipitation community has, in part, been successful in persuading agencies to keep such missions operating after the end of their designed lifetime (e.g., TRMM), with partial failures (e.g., *Megha-Tropiques*), or after station-keeping fuel was exhausted (e.g., *MetOp-A*). The extension of mission lifetimes has only been, and likely will be, an issue for the larger satellite systems.

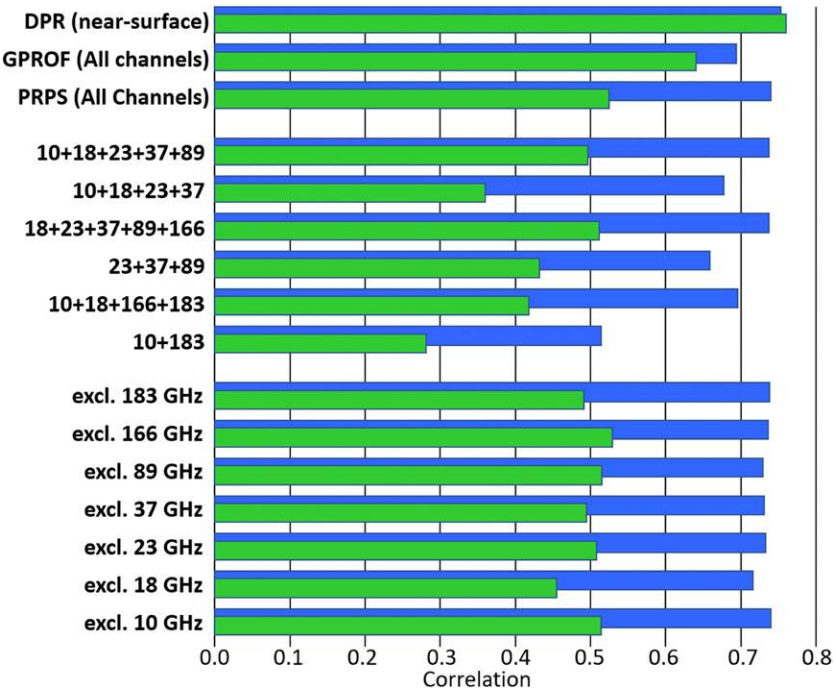


**Fig. 6. Scenarios used to study the effects of channel loss and channel combinations, based upon instantaneous Precipitation Retrieval and Profiling Scheme (PRPS) retrievals from the 13-channel, 7-frequency GMI sensor, compared with surface radar data over the United Kingdom for 2017. The blue bars are for over ocean retrievals, while the green bars are for over land. The top three retrievals (DPR, GPROF, and PRPS, where the last two are computed from GMI) can be used as benchmarks. The exclusion of a single channel has relatively little effect, except for the 18 GHz primarily over land. Generally, the more channels that are available, the better the retrieval as seen in the multifrequency 10–89- or 18–166-GHz retrieval. A narrow frequency range results in poorer performance, particularly at high-frequency channels, although the inclusion of a low-frequency water vapor channel does significantly improve the performance over the ocean.**

***Retrieval scheme resilience.*** Many current retrieval schemes require a full set of observations to generate a precipitation estimate. However, many schemes could still contribute useful information with fewer channels. Figure 6 shows a range of retrieval scenarios using different channel combinations. The loss of a single channel on a diverse-channel sensor, such as the GMI, only degrades the retrieved precipitation marginally. The better performance of precipitation retrievals from the observations gathered over a wide range of frequencies has been shown by Kidd et al. (2018). Additionally, the flexible utilization of channels in the retrievals has particular merit when dealing with surface-based radio-frequency interference (RFI; Wu and Weng 2011), which necessitates the exclusion of certain channels from retrieval schemes at certain times/locations. Furthermore, the calculation of the errors and uncertainties associated with the retrieved precipitation is urgently needed to allow users to assess the usefulness of different retrievals. New techniques should also be investigated and developed that merge observational data before the retrieval stage, rather than merging precipitation estimates postretrieval. The last point might be a longer-term goal, but it is possible to envisage a scenario where two satellites in very similar orbits, both experiencing channel degradation, could jointly provide the capabilities of a single sensor.

***Data availability and access.*** While most precipitation-related satellite observations are freely available both in terms of being available and accessible to any particular user and for that user to share more widely, there are many datasets that are more restrictive and may not be accessible to all potential users. Furthermore, the access to such datasets in very near–real time is of great importance to many user applications, such as flood forecasting, to

ensure timely integration into their processing systems. Crucially, science works best when such data are accessible to the community, as shown by the open release of the DMSP SSMI data in 1987 by the U.S. Department of Defense, which enabled the careers many of the current generation of precipitation scientists and the development of their retrieval schemes.

## Recommendations

Based upon the current precipitation constellation and planned missions, the following course of action is necessary to ensure the long-term continuity of global satellite precipitation observations:

(i) reaffirm commitment and support for current and planned precipitation-capable missions with free and open data sharing by the appropriate agencies and organizations;
(ii) develop a long-term strategy for a viable constellation of precipitation-capable sensors that meet the necessary scientific and user requirements. Specifically,

    1) PMW sensors with diverse channels covering the primary precipitation-sensitive frequencies with good spatial resolution as exemplified by the AMSR/GMI class of sensors, and
    2) operational AMW sensors in a non-Sun-synchronous orbit for cross-calibration and reference standard for PMW (and IR) precipitation estimates, as exemplified by the mapping capabilities of the PR/DPR and the sensitivity of the CPR;

(iii) support the continuation of precipitation-capable missions beyond nominal mission lifetime operations, with due regard for the limitations imposed by deorbiting/sensor degradation considerations;
(iv) integrate new technologies, such as smallsats and cubesats, with access to new datasets where these address the necessary scientific and user requirements; and
(v) implement mitigation strategies within the precipitation retrieval schemes to maximize use of suboptimal observations, including failed/denied channels, to help ensure continuity in adequate sampling.

**Acknowledgments.** The authors acknowledge the formative role in this work that was provided by many colleagues' discussions, presentations, and working group deliberations in the International Precipitation Working Group, the Precipitation Virtual Constellation working group of the Committee on Earth Observation Satellites, the Integrated Global Water Cycle Observations community of practice, and many specialty conference sessions. Funding for Kidd is in part from the NASA/GSFC-UMD/ESSIC Cooperative Agreement, NASA Grant NNX17AE79A.

## References


Accadia, C., V. Mattioli, P. Colucci, P. Schlüssel, S. D'Addio, U. Klein, T. Wehr, and C. Donlon, 2020: Microwave and sub-mm wave sensors: A European perspective. *Satellite Precipitation Measurement*, V. Levizzani et al., Eds., Advances in Global Change Research, Vol. 67, Springer, 83–97, https://doi.org/10.1007/978-3-030-24568-9_5.

Adler, R. F., and Coauthors, 2003: The version-2 Global Precipitation Climatology Project (GPCP) monthly precipitation analysis (1979–present). *J. Hydrometeor.*, **4**, 1147–1167, https://doi.org/10.1175/1525-7541(2003)004<1147:TVGPCP>2.0.CO;2.

——, G. Gu, M. Sapiano, J. J. Wang, and G. J. Huffman, 2017: Global precipitation: Means, variations and trends during the satellite era (1979–2014). *Surv. Geophys.*, **38**, 679–699, https://doi.org/10.1007/s10712-017-9416-4.

Bagaglini, L., P. Sanò, D. Casella, E. Cattani, and G. Panegrossi, 2021: The Passive microwave Neural network Precipitation Retrieval algorithm for climate applications (PNPR-CLIM): Design and verification. *Remote Sens.* **13**, 1701, https://doi.org/10.3390/rs13091701.

Battaglia, A., and Coauthors, 2020: Space-borne cloud and precipitation radars: Status, challenges and ways forward. *Rev. Geophys.*, **58**, e2019RG000686, https://doi.org/10.1029/2019RG000686.

Behrangi, A., 2020: Improving High-latitude and cold region precipitation analysis. *Satellite Precipitation Measurement*, V. Levizzani et al., Eds., Advances in Global Change Research, Vol. 67, Springer, 881–895, https://doi.org/10.1007/978-3-030-35798-6_21.

Bizzarri, B., and Coauthors, 2002: Requirements and perspectives for MW/sub-mm sounding from geostationary satellite. *Proc. of the EUMETSAT Meteorological Satellite Conf.*, Dublin, Ireland, EUMETSAT, 97–105.

Blackwell, W. J., and Coauthors, 2018: An overview of the TROPICS NASA Earth Venture Mission. *Quart. J. Roy. Meteor. Soc.*, **144**, 16–26, https://doi.org/10.1002/qj.3290.

Brocca, L., and Coauthors, 2014: Soil as a natural rain gauge: Estimating global rainfall from satellite soil moisture data. *J. Geophys. Res. Atmos.*, **119**, 5128–5141, https://doi.org/10.1002/2014JD021489.

Campos, E., and I. Zawadzki, 2000: Instrumental uncertainties in *Z–R* relations. *J. Appl. Meteor.*, **39**, 1088–1102, https://doi.org/10.1175/1520-0450(2000)039<1088:IUIZRR>2.0.CO;2.

Chambon, P., R. Roca, I. Jobard, and M. Capderou, 2013: The sensitivity of tropical rainfall estimation from satellite to the configuration of the microwave imager constellation. *IEEE Geosci. Remote Sens. Lett.*, **10**, 996–1000, https://doi.org/10.1109/LGRS.2012.2227668.

——, S. Q. Zhang, A. Y. Hou, M. Zupanski, and S. Cheung, 2014: Assessing the impact of pre-GPM microwave precipitation observations in the Goddard WRF ensemble data assimilation system. *Quart. J. Roy. Meteor. Soc.*, **140**, 1219–1235, https://doi.org/10.1002/qj.2215.

Ciach, G. J., 2003: Local random errors in tipping-bucket rain gauge measurements. *J. Atmos. Oceanic Technol.*, **20**, 752–759, https://doi.org/10.1175/1520-0426(2003)20<752:LREITB>2.0.CO;2.

——, and W. F. Krajewski, 1999: Radar–rain gauge comparisons under observational uncertainties. *J. Appl. Meteor.*, **38**, 1519–1525, https://doi.org/10.1175/1520-0450(1999)038<1519:RRGCUO>2.0.CO;2.

Crowther, R., 2002: Space junk–protecting space for future generations. *Science*, **296**, 1241–1242, https://doi.org/10.1126/science.1069725.

Duchon, C. E., and G. R. Essenberg, 2001: Comparative rainfall observations from pit and aboveground rain gauges with and without wind shields. *Water Resour. Res.*, **37**, 3253–3263, https://doi.org/10.1029/2001WR000541.

——, and C. J. Biddle, 2010: Undercatch of tipping-bucket gauges in high rain rate events. *Adv. Geosci.*, **25**, 11–15, https://doi.org/10.5194/adgeo-25-11-2010.

Duruisseau, F., and Coauthors, 2017: Investigating the potential benefit to a mesoscale NWP model of a microwave sounder on board a geostationary satellite. *Quart. J. Roy. Meteor. Soc.*, **143**, 2104–2115, https://doi.org/10.1002/qj.3070.

Eriksson, P., B. Rydberg, V. Mattioli, A. Thoss, C. Accadia, U. Klein, and S. Buehler, 2020: Towards an operational Ice Cloud Imager (ICI) retrieval product. *Atmos. Meas. Tech.*, **13**, 53–71, https://doi.org/10.5194/amt-13-53-2020.

Forster, J., 1994: Rain measurement on buoys using hydrophones. *IEEE J. Oceanic Eng.*, **19**, 23–29, https://doi.org/10.1109/48.289446.

Friedl, L., 2014: GEO Task US-09-01a: Critical Earth observation priorities; Precipitation data characteristics and user types. Group on Earth Observations, 60 pp., https://sbageotask.larc.nasa.gov/GEO%20US0901a%20-%20Precipitatio%20Data%20Report%20-%20Final.pdf.

Goldberg, M. D., H. Kilcoyne, H. Cikanek, and A. Mehta, 2013: Joint Polar Satellite System: The United States next generation civilian polar-orbiting environmental satellite system. *J. Geophys. Res. Atmos.*, **118**, 13 463–13 475, https://doi.org/10.1002/2013JD020389.

Guo, Y., N. M. Lu, C. L. Qi, S. Y. Gu, and J. M. Xu, 2015: Calibration and validation of microwave humidity and temperature sounder onboard FY-3C satellite. *Chin. J. Geophys.*, **58**, 20–31.

Harrison, D. L., S. J. Driscoll, and M. Kitchen, 2000: Improving precipitation estimates from weather radar using quality control and correction techniques. *Meteor. Appl.*, **7**, 135–144, https://doi.org/10.1017/S1350482700001468.

Herold, N., L. V. Alexander, M. G. Donat, S. Contractor, and A. Becker, 2016: How much does it rain over land? *Geophys. Res. Lett.*, **43**, 341–348, https://doi.org/10.1002/2015GL066615.

Hou, A. Y., and Coauthors, 2014: The Global Precipitation Measurement mission. *Bull. Amer. Meteor. Soc.*, **95**, 701–722, https://doi.org/10.1175/BAMS-D-13-00164.1.

Huffman, G. J., and Coauthors, 2007: The TRMM Multisatellite Precipitation Analysis (TMPA): Quasi-global, multiyear, combined-sensor precipitation estimates at fine scales. *J. Hydrometeor.*, **8**, 38–55, https://doi.org/10.1175/JHM560.1.

——, and Coauthors, 2020: Integrated Multi-satellite Retrievals for the Global Precipitation Measurement (GPM) Mission (IMERG). *Satellite Precipitation Measurement*, V. Levizzani et al., Eds., Advances in Global Change Research, Vol. 67, Springer, 343–353, https://doi.org/10.1007/978-3-030-24568-9_19.

Imaoka, K., and Coauthors, 2010: Global Change Observation Mission (GCOM) for monitoring carbon, water cycles, and climate change. *Proc. IEEE*, **98**, 717–734, https://doi.org/10.1109/JPROC.2009.2036869.

Janowiak, J. E., R. J. Joyce, and Y. Yarosh, 2001: A real-time global half-hourly pixel-resolution infrared dataset and its applications. *Bull. Amer. Meteor. Soc.*, **82**, 205–218, https://doi.org/10.1175/1520-0477(2001)082<0205:ARTGHH>2.3.CO;2.

Joyce, R. J., and P. Xie, 2011: Kalman filter–based CMORPH. *J. Hydrometeor.*, **12**, 1547–1563, https://doi.org/10.1175/JHM-D-11-022.1.

Kasahara, M., M. Kachi, K. Inaoka, H. Fujii, T. Kubota, R. Shimada, and Y. Kojima, 2020: Overview and current status of GOSAT-GW mission and AMSR3 instrument. *Proc. SPIE*, **11530**, 1153007, https://doi.org/10.1117/12.2573914.

Kidd, C., and C. Muller, 2010: The combined passive microwave-infrared (PMIR) algorithm. *Satellite Rainfall Applications for Surface Hydrology*, F. Hossain and M. Gebremichael, Eds., Springer, 69–83, https://doi.org/10.1007/978-90-481-2915-7_5.

——, and V. Levizzani, 2011: Status of satellite precipitation retrievals. *Hydrol. Earth Syst. Sci.*, **15**, 1109–1116, https://doi.org/10.5194/hess-15-1109-2011.

——, and ——, 2019: Quantitative precipitation estimation from satellite observations. *Extreme Hydroclimatic Events and Multivariate Hazards in a Changing Climate*, V. Maggioni and C. Massari, Eds., Elsevier, 3–39, https://doi.org/10.1016/B978-0-12-814899-0.00001-8.

——, T. Matsui, J. Chern, K. Mohr, C. Kummerow, and D. Randel, 2016: Global precipitation estimates from cross-track passive microwave observations using a physically based retrieval scheme. *J. Hydrometeor.*, **17**, 383–400, https://doi.org/10.1175/JHM-D-15-0051.1.

——, A. Becker, G. J. Huffman, C. L. Muller, P. Joe, G. Skofronick-Jackson, and D. B. Kirschbaum, 2017: So, how much of the Earth's surface is covered by rain gauges? *Bull. Amer. Meteor. Soc.*, **98**, 69–78, https://doi.org/10.1175/BAMS-D-14-00283.1.

——, J. Tan, P.-E. Kirstetter, and W. A. Petersen, 2018: Validation of the Version 05 Level 2 precipitation products from the GPM Core Observatory and constellation satellite sensors. *Quart. J. Roy. Meteor. Soc.*, **144**, 313–328, https://doi.org/10.1002/qj.3175.

——, Y. N. Takayabu, G. M. Skofronick-Jackson, G. J. Huffman, S. A. Braun, T. Kubota, and F. J. Turk, 2020: The Global Precipitation Measurement (GPM) mission. *Satellite Precipitation Measurement*, V. Levizzani et al., Eds., Advances in Global Change Research, Vol. 67, Springer, 3–23, https://doi.org/10.1007/978-3-030-24568-9_1.

——, T. Matsui, and S. Ringerud, 2021: Precipitation retrievals from passive microwave cross-track sensors: The precipitation retrieval and profiling scheme. *Remote Sens.*, **13**, 947, https://doi.org/10.3390/rs13050947.

Kirschbaum, D. B., and Coauthors, 2017: NASA's remotely sensed precipitation: A reservoir for applications users. *Bull. Amer. Meteor. Soc.*, **98**, 1169–1184, https://doi.org/10.1175/BAMS-D-15-00296.1.

Knapp, K. R., and S. L. Wilkins, 2018: Gridded satellite (GridSat) GOES and CONUS data. *Earth Syst. Sci. Data*, **10**, 1417–1425, https://doi.org/10.5194/essd-10-1417-2018.

Kochendorfer, J., and Coauthors, 2017: The quantification and correction of wind-induced precipitation measurement errors. *Hydrol. Earth Syst. Sci.*, **21**, 1973–1989, https://doi.org/10.5194/hess-21-1973-2017.

Kubota, T., and Coauthors, 2020: Global Satellite Mapping of Precipitation (GSMaP) products in the GPM era. *Satellite Precipitation Measurement*, V. Levizzani et al., Eds., Advances in Global Change Research, Vol. 67, Springer, 355–373, https://doi.org/10.1007/978-3-030-24568-9_20.

Kummerow, C. D., 2020: Introduction to passive microwave retrieval methods. *Satellite Precipitation Measurement*, V. Levizzani et al., Eds., Advances in Global Change Research, Vol. 67, Springer, 123–140, https://doi.org/10.1007/978-3-030-24568-9_7.

——, W. Barnes, T. Kozu, J. Shiue, and J. Simpson, 1998: The Tropical Rainfall Measuring Mission (TRMM) sensor package. *J. Atmos. Oceanic Technol.*, **15**, 809–817, https://doi.org/10.1175/1520-0426(1998)015<0809:TTRMMT>2.0.CO;2.

Kundzewicz, Z. W., and Coauthors, 2014: Flood risk and climate change: Global and regional perspectives. *Hydrol. Sci. J.*, **59**, 1–28, https://doi.org/10.1080/02626667.2013.857411.

Kyriakidis, P. C., J. Kim, and N. L. Miller, 2001: Geostatistical mapping of precipitation from rain gauge data using atmospheric and terrain characteristics. *J. Appl. Meteor.*, **40**, 1855–1877, https://doi.org/10.1175/1520-0450(2001)040<1855:GMOPFR>2.0.CO;2.

Lambrigtsen, B., 2019: Observing clouds, convection and precipitation with a geostationary microwave sounder. *2019 IEEE Int. Geoscience and Remote Sensing Symp.*, Yokohama, Japan, IEEE, 7548–7551, https://doi.org/10.1109/IGARSS.2019.8899826.

——, S. T. Brown, S. J. Dinardo, T. C. Gaier, P. P. Kangaslahti, and A. B. Tanner, 2007: GeoSTAR–A geostationary microwave sounder for the future. NASA Doc., 11 pp., https://trs.jpl.nasa.gov/bitstream/handle/2014/41287/07-2264.pdf.

Lawrence, H., N. Bormann, A. Geer, Q. Lu, and S. J. English, 2018: Evaluation and assimilation of the microwave sounder MWHS-2 onboard FY-3C in the ECMWF Numerical Weather Prediction system. *IEEE Trans. Geosci. Remote Sens.*, **56**, 3333–3349, https://doi.org/10.1109/TGRS.2018.2798292.

Leijnse, H., R. Uijlenhoet, and J. N. M. Stricker, 2007: Rainfall measurement using radio links from cellular communication networks. *Water Resour. Res.*, **43**, W03201, https://doi.org/10.1029/2006WR005631.

Levizzani, V., and Coauthors, 2018: The activities of the International Precipitation Working Group. *Quart. J. Roy. Meteor. Soc.*, **144**, 3–15, https://doi.org/10.1002/qj.3214.

Li, N., J. He, S. Zhang, and N. Lu, 2018: Precipitation retrieval using 118.75-GHz and 183.31-GHz channels from MWHTS on FY-3C satellite. *IEEE J. Sel. Top. Appl. Earth Obs. Remote Sens.*, **11**, 4373–4389, https://doi.org/10.1109/JSTARS.2018.2873255.

Luini, L., and C. Capsoni, 2012: The impact of space and time averaging on the spatial correlation of rainfall. *Radio Sci.*, **47**, RS3013, https://doi.org/10.1029/2011RS004915.

Lundquist, J., M. Hughes, E. Gutmann, and S. Kapnick, 2019: Our skill in modeling mountain rain and snow is bypassing the skill of our observational networks. *Bull. Amer. Meteor. Soc.*, **100**, 2473–2490, https://doi.org/10.1175/BAMS-D-19-0001.1.

Ma, B. B., and J. A. Nystuen, 2005: Passive acoustic detection and measurement of rainfall at sea. *J. Atmos. Oceanic Technol.*, **22**, 1225–1248, https://doi.org/10.1175/JTECH1773.1.

Medwin, H., J. A. Nystuen, P. W. Jacobus, L. H. Ostwald, and D. E. Snyder, 1992: The anatomy of underwater rain noise. *J. Acoust. Soc. Amer.*, **92**, 1613–1623, https://doi.org/10.1121/1.403902.

Michelson, D. B., 2004: Systematic correction of precipitation gauge observations using analyzed meteorological variables. *J. Hydrol.*, **290**, 161–177, https://doi.org/10.1016/j.jhydrol.2003.10.005.

Mimikou, M. A., and E. A. Baltas, 1996: Flood forecasting based on radar rainfall measurements. *J. Water Resour. Plann. Manage.*, **122**, 151, https://doi.org/10.1061/(ASCE)0733-9496(1996)122:3(151).

Mo, T., 1995: A study of the microwave sounding unit on the NOAA-12 satellite. *IEEE Trans. Geosci. Remote Sens.*, **33**, 1141–1152, https://doi.org/10.1109/36.469478.

Newell, D., D. Draper, Q. Remund, B. Woods, C. Mays, B. Bensler, D. Miller, and K. Eastman, 2020: Weather Satellite Follow-On–Microwave (WSF-M) design and predicted performance. *20th Symp. on Meteorological Observation and Instrumentation*, Boston, MA, Amer. Meteor. Soc., 7.1, https://ams.confex.com/ams/2020Annual/webprogram/Paper369912.html.

Overeem, A., H. Leijnse, and R. Uijlenhoet, 2011: Measuring urban rainfall using microwave links from commercial cellular communication networks. *Water Resour. Res.*, **47**, W12505, https://doi.org/10.1029/2010WR010350.

Pumphrey, H. C., L. A. Crum, and L. Bjømø, 1989: Underwater sound produced by individual drop impacts and rainfall. *J. Acoust. Soc. Amer.*, **85**, 1518–1526, https://doi.org/10.1121/1.397353.

Reed, P. M., N. W. Chaney, J. D. Herman, M. P. Ferringer, and E. F. Wood, 2015: Internationally coordinated multi-mission planning is now critical to Sustain the space-based rainfall observations needed for managing floods globally. *Environ. Res. Lett.*, **10**, 024010, https://doi.org/10.1088/1748-9326/10/2/024010.

Roca, R., and Coauthors, 2015: The Megha-Tropiques mission: A review after three years in orbit. *Front. Earth Sci.*, **3**, 1–14, https://doi.org/10.3389/feart.2015.00017.

——, and Coauthors, 2018: Quantifying the contribution of the Megha-Tropiques mission to the estimation of daily accumulated rainfall in the Tropics. *Quart. J. Roy. Meteor. Soc.*, **144**, 49–63, https://doi.org/10.1002/qj.3327.

Semplak, R. A., and R. H. Turrin, 1969: Some measurements of attenuation by rainfall at 18.5 GHz. *Bell Syst. Tech. J.*, **48**, 1767–1787, https://doi.org/10.1002/j.1538-7305.1969.tb01151.x.

Sevruk, B., 2005: Rainfall measurement: Gauges. *Encyclopedia of Hydrological Sciences*, M.G. Anderson, Ed., John Wiley & Sons Ltd, 529–536.

——, and S. Klemm, 1989: Catalogue of National Standard Precipitation Gauges. Instruments and Observing Methods Rep. 39, WMO/TD No. 313, World Meteorological Organization, 50 pp., https://library.wmo.int/doc_num.php?explnum_id=9514.

Simpson, J. R., R. F. Adler, and G. R. North, 1988: A proposed Tropical Rainfall Measuring Mission (TRMM) satellite. *Bull. Amer. Meteor. Soc.*, **69**, 278–295, https://doi.org/10.1175/1520-0477(1988)069<0278:APTRMM>2.0.CO;2.

Skofronick-Jackson, G., and Coauthors, 2017: The Global Precipitation Measurement (GPM) mission for science and society. *Bull. Amer. Meteor. Soc.*, **98**, 1679–1695, https://doi.org/10.1175/BAMS-D-15-00306.1.

——, M. Kulie, L. Milani, S. J. Munchak, N. B. Wood, and V. Levizzani, 2019: Satellite estimation of falling snow: A Global Precipitation Measurement (GPM) Core Observatory perspective. *J. Appl. Meteor. Climatol*, **58**, 1429–1448, https://doi.org/10.1175/JAMC-D-18-0124.1.

Stephens, G. L., and Coauthors, 2002: The CloudSat mission and the A-Train: A new dimension of space-based observations of clouds and precipitation. *Bull. Amer. Meteor. Soc.*, **83**, 1771–1790, https://doi.org/10.1175/BAMS-83-12-1771.

——, D. Winker, J. Pelon, C. Trepte, D. Vane, C. Yuhas, T. L'Ecuyer, and M. Lebsock, 2018: CloudSat and CALIPSO within the A-train: Ten years of actively observing the Earth system. *Bull. Amer. Meteor. Soc.*, **99**, 569–581, https://doi.org/10.1175/BAMS-D-16-0324.1.

——, and Coauthors, 2020: The emerging technological revolution in Earth observations. *Bull. Amer. Meteor. Soc.*, **101**, E274–E285, https://doi.org/10.1175/BAMS-D-19-0146.1.

Strangeways, I. C., 2004: Improving precipitation measurement. *Int. J. Climatol.*, **24**, 1443–1460, https://doi.org/10.1002/joc.1075.

Sun, Y., S. Solomon, A. Dai, and R. W. Portmann, 2006: How often does it rain? *J. Climate*, **19**, 916–934, https://doi.org/10.1175/JCLI3672.1.

Tanner, A. B., and Coauthors, 2007: Initial results of the Geostationary Synthetic Thinned Array Radiometer. *IEEE Trans. Geosci. Remote Sens.*, **45**, 1947–1957, https://doi.org/10.1109/TGRS.2007.894060.

Tapiador, F. J., and Coauthors, 2011: Global precipitation measurement: Methods, datasets and applications. *Atmos. Res.*, **104–105**, 70–97, https://doi.org/10.1016/j.atmosres.2011.10.021.

Thériault, J. M., R. Rasmussen, K. Ikeda, and S. Landolt, 2012: Dependence of snow gauge collection efficiency on snowflake characteristics. *J. Appl. Meteor. Climatol.*, **51**, 745–762, https://doi.org/10.1175/JAMC-D-11-0116.1.

Trenberth, K. E., J. T. Fasullo, and J. Kiehl, 2009: Earth's global energy budget. *Bull. Amer. Meteor. Soc.*, **90**, 311–324, https://doi.org/10.1175/2008BAMS2634.1.

Uijlenhoet, R., 2001: Raindrop size distributions and radar reflectivity-rain rate relationships for radar hydrology. *Hydrol. Earth Syst. Sci.*, **5**, 615–628, https://doi.org/10.5194/hess-5-615-2001.

——, M. Steiner, and J. A. Smith, 2003: Variability of raindrop size distributions in a squall line and implications for radar rainfall estimation. *J. Hydrometeor.*, **4**, 43–61, https://doi.org/10.1175/1525-7541(2003)004<0043:VORSDI>2.0.CO;2.

Vicente-Serrano, S. M., S. Beguería, and J. I. López-Moreno, 2010: A multiscalar drought index sensitive to global warming: The standardized precipitation evapotranspiration index. *J. Climate*, **23**, 1696–1718, https://doi.org/10.1175/2009JCLI2909.1.

Villarini, G., P. V. Mandapaka, W. F. Krajewski, and R. J. Moore, 2008: Rainfall and sampling uncertainties: A rain gauge perspective. *J. Geophys. Res.*, **113**, D11102, https://doi.org/10.1029/2007JD009214.

Wentz, F. J., and D. Draper, 2016: On-orbit absolute calibration of the global precipitation measurement microwave imager. *J. Atmos. Oceanic Technol.*, **33**, 1393–1412, https://doi.org/10.1175/JTECH-D-15-0212.1.

Whiton, R. C., P. L. Smith, S. G. Bigler, K. E. Wilk, and A. C. Harbuck, 1998a: History of operational use of weather radar by U.S. Weather Services. Part I: The Pre-NEXRAD era. *Wea. Forecasting*, **13**, 219–243, https://doi.org/10.1175/1520-0434(1998)013<0219:HOOUOW>2.0.CO;2.

——, ——, ——, ——, and ——, 1998b: History of operational use of weather radar by U.S. Weather Services. Part II: Development of operational Doppler weather radars. *Wea. Forecasting*, **13**, 244–252, https://doi.org/10.1175/1520-0434(1998)013<0244:HOOUOW>2.0.CO;2.

Witze, A., 2018: The quest to conquer Earth's space junk problem. *Nature*, **561**, 24–26, https://doi.org/10.1038/d41586-018-06170-1.

Wu, Y., and F. Weng, 2011: Detection and correction of AMSR-E radio-frequency interference. *Acta Meteor. Sin.*, **25**, 669–681, https://doi.org/10.1007/s13351-011-0510-0.

Zhang, J., and Coauthors, 2011: National Mosaic and Multi-sensor QPE (NMQ) system: Description, results, and future plans. *Bull. Amer. Meteor. Soc.*, **92**, 1321–1338, https://doi.org/10.1175/2011BAMS-D-11-00047.1.

——, and Coauthors, 2016: Multi-Radar Multi-Sensor (MRMS) Quantitative Precipitation Estimation: Initial Operating Capabilities. *Bull. Amer. Meteor. Soc.*, **97**, 621–638, https://doi.org/10.1175/BAMS-D-14-00174.1.